SINTEF

TECHNICAL REPORT

SINTEF Energy Research

Address: NO-7465 Trondheim NORWAY
Reception: Sem Sælands vei 11
Telephone: + 47 73 59 72 00
Telefax: + 47 73 59 72 50

www.energy.sintef.no

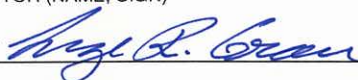Enterprise No.: NO 939 350 675 MVA

SUBJECT/TASK (title)

Characterisation studies on peat

CONTRIBUTOR(S)

Øyvind Skreiberg and Alexandra Skreiberg

CLIENT(S)

The KRAV project consortium

TR NO.	DATE	CLIENT'S REF.		PROJECT NO.
TR A6901	2009-12-01			16X807

EL. FILE CODE	REPORT TYPE	RESPONSIBLE (NAME, SIGN.)		CLASSIFICATION
		Øyvind Skreiberg		Unrestricted

ISBN NO.	RESEARCH DIRECTOR (NAME, SIGN)		COPIES	PAGES
978-82-594-3429-6	Inge R. Gran			20

DIVISION	LOCATION	LOCAL FAX
Energy Processes	Kolbjørn Hejes vei 1A	+ 47 73 59 28 89

RESULT (summary)

Experiments with peat supplied by the KRAV industry partner Eidsiva Bioenergi AS have been carried out with the aim of characterisation of the peat. The characterisation includes ultimate and proximate analysis of peat pellets, TGA experiments and multi-fuel reactor experiments. Main results are presented and discussed.

KEYWORDS

SELECTED BY AUTHOR(S)

Biomass	TGA
Combustion	Pyrolysis

SINTEF

TABLE OF CONTENTS

Page

1 THE PEAT

Peat is an inhomogeneous complex material with a natural variation in botanical origin and chemical and physical composition. Even peat is not internationally classified as biomass its properties and combustion behaviour are similar to that of biomass, since it is organic matter. The potential applications for energetic recovery from peat must take into account the specific characteristic of peat compared to biomass [1,2,3,4,5]. Figure 1 shows the atomic H/C and O/C ratio of different types of carbonaceous fuels in a van Krevelen diagram.
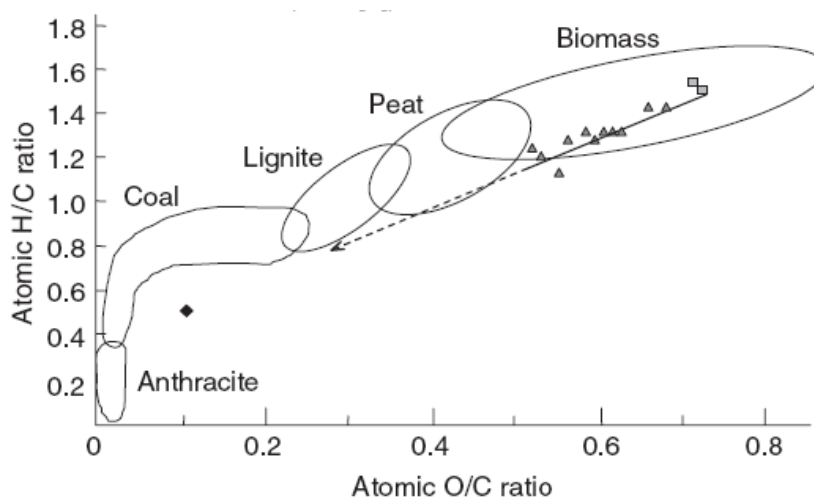

Figure 1 Van Krevelen diagram [4]

From the van Krevelen diagram follows that peat has higher carbon and hydrogen content compared to biomass.

As the content of peat may vary, prior to using it as a fuel, an ultimate and proximate analysis should be carried out. The virgin peat used in the experimental work was supplied by Eidsiva Bioenergi AS. Ultimate and proximate analyses of the peat pellets made from dried and milled virgin peat are reported in Table 1. As expected, the peat has a higher carbon and hydrogen content than biomass, while the nitrogen content is similar to some biomass waste fractions, e.g. coffee waste, i.e. rather high. The sulphur and chlorine level is in the same range as for some non-woody biomass fuels. The fixed carbon content of the peat is higher than for biomass while the volatile content is lower. The ash amount is similar to some biomass waste fractions.

Table 1 Properties of peat pellets tested

Fuel	Ultimate analysis (wt%, dry ash free basis)						Moisture (wt%, wb)	Proximate analysis (wt%, db)		
	C	H	O	N	S	Cl		Ash	Volatiles	Fixed C
Peat pellets	53.62	7.04	bd	2.92	0.068	0.098	25.9	2	74.0	24

bd: by difference; wb: wet basis; db: dry basis

The peat pellets used in experimental work are shown in Figure 2.

Figure 2 Peat pellets

2 TGA EXPERIMENTS

Thermogravimetric analysis of the peat pellets was performed using a thermobalance, a Mettler Toledo TGA/SDTA 8951E, as Figure 3 shows (the mass spectrometry (MS) option was not used in this analysis due to lack of adequate MS calibration).
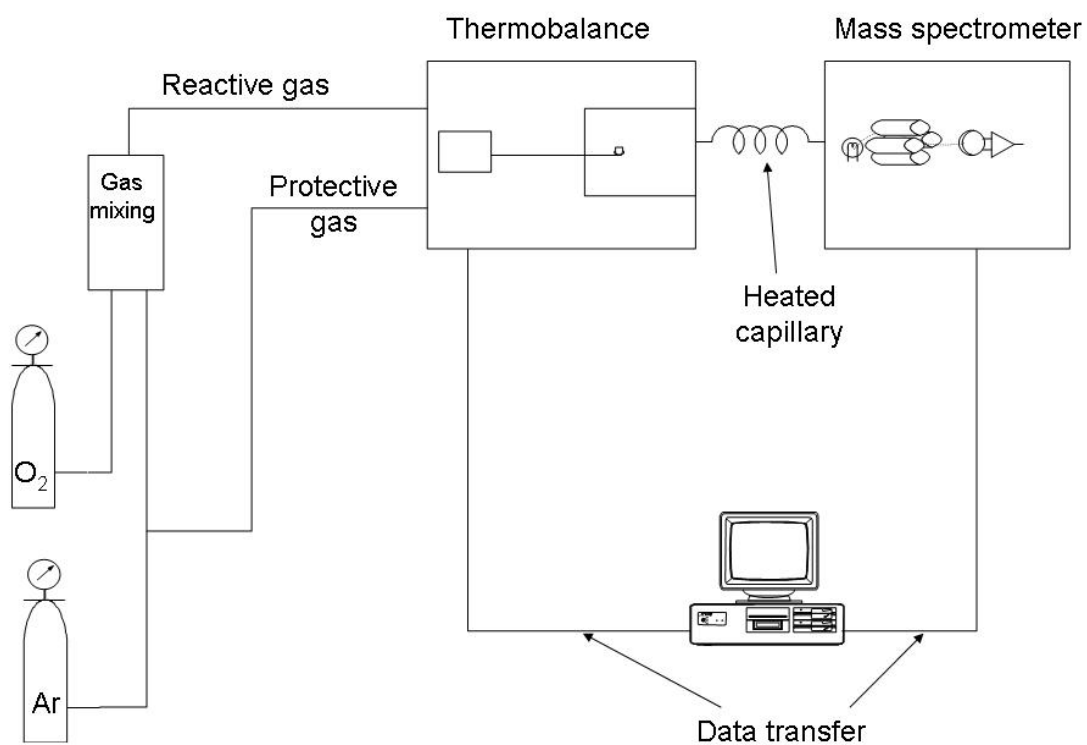

Figure 3 TGA-MS instrumentation

Two sets of thermogravimetric experiments have been carried out:
- pyrolysis under inert atmosphere/reaction gas 100 % argon
- combustion under oxidative atmosphere/reaction gas composition 21 vol% oxygen + 79 vol% argon

Samples were grinded to powder and placed into alumina pan. The heating rate was controlled at 5 K/min, 20 K/min and 40 K/min from 60 °C to 900 °C. The flow rate of the reactive gas was 100 mL/min. The purge gas was argon at flow rate of 20 mL/min.

During the experiments weight loss was monitored by the TGA. Figure 4 and Figure 5 shows TGA results at pyrolysis and combustion conditions for the three heating rates. As expected, an increasing heating rate delays the temperature onset for devolatilisation but increases the peak devolatilisation rate, both at pyrolysis and combustion conditions. Comparing pyrolysis and combustion conditions, devolatilisation at combustion conditions starts at a slightly lower temperature, and the peak devolatilisation rate is higher. At higher temperatures the carbon will oxidise at combustion conditions, with only ash remaining, while ash and fixed carbon remains at pyrolysis conditions.
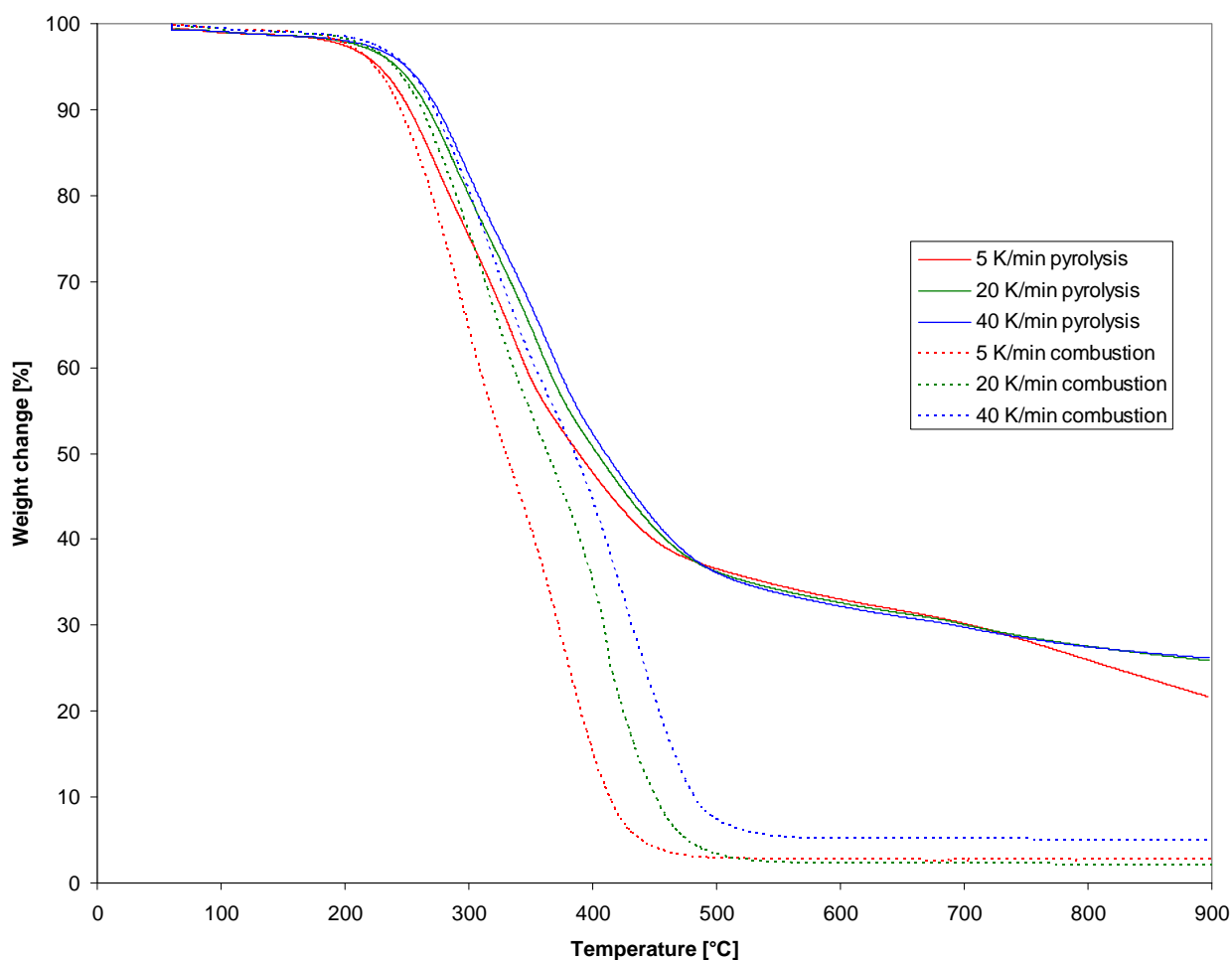

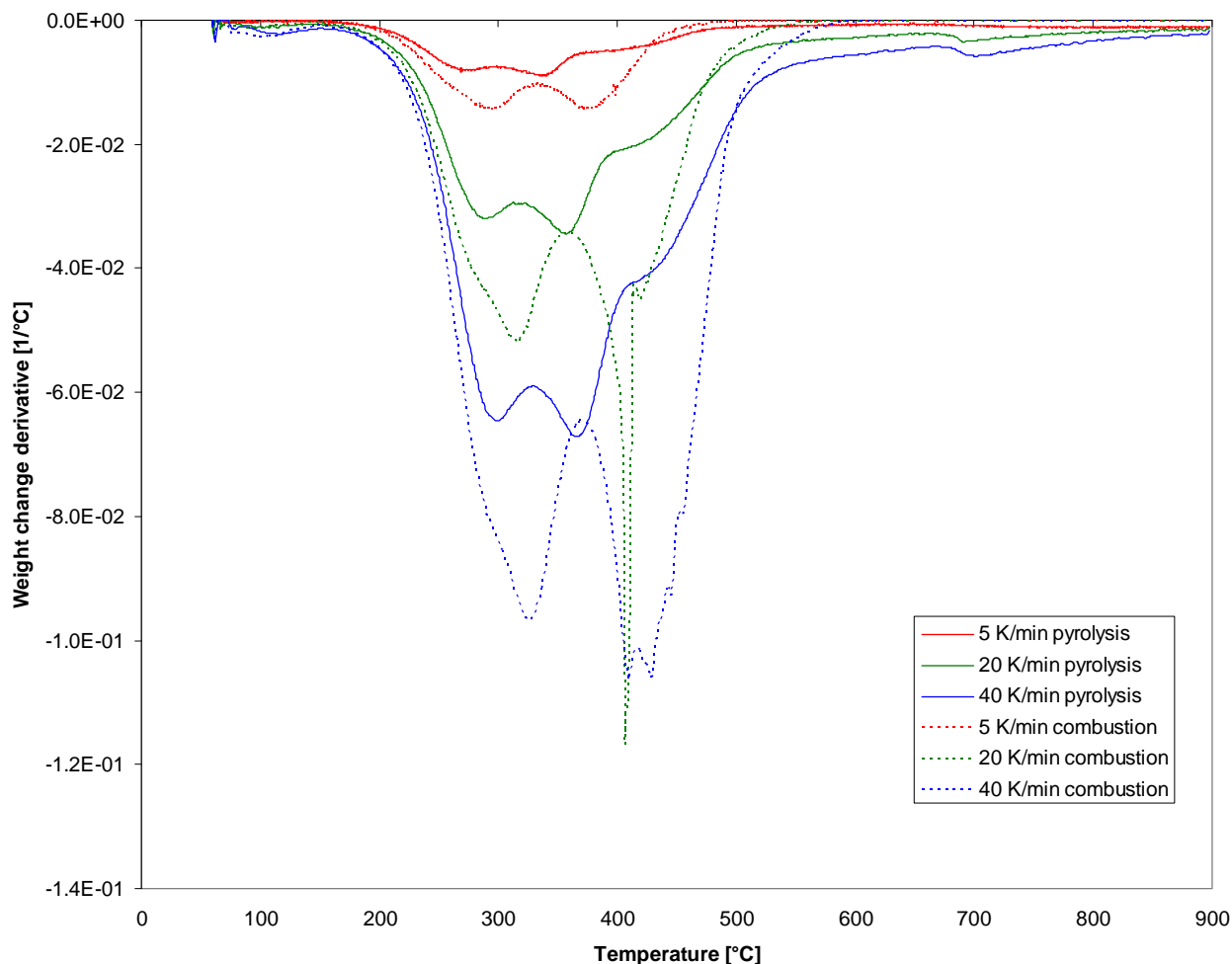**Figure 4 Pyrolysis and combustion weight change in the TGA with 5 mg samples. Effect of heating rate**

Figure 5 Pyrolysis and combustion weight change derivative in the TGA with 5 mg samples. Effect of heating rate

3   MULTI-FUEL REACTOR EXPERIMENTS

Multi-fuel reactor experiments were carried out in the multi-fuel reactor setup at SINTEF Energy Research. The Monika 1 reactor shown in Figure 6 was used in the experiments. The multi-fuel reactor setup is described in detail in [6]. Experiments were carried out at reactor temperatures of 750, 800, 850 and 900 °C. The fuel feeding rate was kept constant at 200 g/h, while at each reactor temperature the air flow was set to achieve four levels of oxygen concentration in the flue gas, i.e. to reveal the influence of excess air ratio. The reactor residence time was from 18 seconds, with the lowest residence time for the highest excess air ratio at the highest reactor temperature.

Flue gas analysis of CO_2, CO, NOx ($NO+NO_2$) and O_2, has been performed using a Horiba portable multi-species gas analyzer, PG-200 series. This was selected since the experiments were combustion experiments and since fast analyzer response time was considered needed. Data were saved to a file every 2 seconds. The measurement ranges used and the measurement uncertainties are shown in Table 2.

Table 2 Gas analysis measurement ranges and uncertainties (Horiba)

Gas species	Measuring principle	Measurement range used	Measurement uncertainty (of full scale)
CO_2	infrared	0-20 %	0.5 %
CO	infrared	0-5000 ppm	0.5 %
NOx (NO+NO_2)	chemiluminescence	0-250 ppm	0.5 %
O_2	paramagnetic	0-25 %	0.5 %

Linearity: 2 % of full scale; Zero and span drift: within 1 % of full scale/day; T90 response speed: within 45 seconds.

Additionally, a portable FTIR was used (Gasmet DX-Series), which also has an integrated (zirconium oxide) O_2 analyzer. The species measured, their measurement ranges and measurement uncertainty are shown in Table 3. The data analysis interval was about 60 seconds.

Table 3 Gas analysis measurement ranges and uncertainties (FTIR)

Gas species	Measurement range	Unit	Measurement uncertainty (of full scale)
H_2O	0-25	vol% wet	2 %
CO_2	0-20	vol% wet	2 %
CO (high range)	0-2	vol% wet	2 %
CO (low range)	0-500	ppm wet	2 %
NO	0-200	ppm wet	2 %
N_2O	0-50	ppm wet	2 %
NO_2	0-100	ppm wet	2 %
SO_2	0-100	ppm wet	2 %
NH_3	0-50	ppm wet	2 %
HCl	0-50	ppm wet	2 %
HF	0-20	ppm wet	2 %
CH_4	0-100	ppm wet	2 %
C_2H_6	0-50	ppm wet	2 %
C_2H_4	0-50	ppm wet	2 %
C_3H_8	0-50	ppm wet	2 %
C_6H_{14}	0-50	ppm wet	2 %
CHOH	0-50	ppm wet	2 %
HCN	0-100	ppm wet	2 %
O_2 (zirconium oxide)	25	vol% dry	2.5 %

System overview

Key data:
up to 1100 °C
ID: 195 mm, H: 2 m
35 + 8 + 2*4.5 = 52 kW
up to 1.2 kg fuel/h
up to 260 Nl air/min

Key data:
up to 1300 °C
ID: 100 mm, H: 2 m
16 + 4 + 4*3 = 32 kW
up to 0.5 kg fuel/h
up to 120 Nl air/min

Flue gas suction system

Scale

Gas analysis

FTIR, GC, Horiba

Heated reactor

View glass

Fuel feeding

Preheater

2 preheaters

Rotating grate

Ash

Monika II

Control

Logging

Impactor

Heated filter

Platform

Gas bottles, pressurised air, and steam generator

FC panel

FC panel

2 preheaters

2 preheaters

Rotating grate

Preheater

Gas analysis

FTIR, GC, Horiba

Heated reactor

View glass

Fuel feeding

Logging

Control

Ash

Monika I

Figure 6 The multi-fuel reactor setup at SINTEF Energy Research

The mass balance of carbon was checked at all data points through comparison of the measured and a calculated CO_2 emission level for both gas analysers. Only data points that satisfied a maximum relative deviation (15 %) between these two values was included in the final results. Additionally, a constraint was set on how fast the excess air ratio was allowed to change from one data point to the next (1 % per second), to remove the data points most likely to be significantly influenced by transient effects. Mass balance calculations were carried out both for carbon and hydrogen, and are shown in Figure 7 and Figure 8 as a function of time for the FTIR analyser. Good agreement was achieved between the measured and calculated CO_2 level in the flue gas (for both analysers), and between the measured and calculated H_2O level (for the FTIR). Calculation of the conversion factors for fuel N, S and Cl to gaseous emissions were also carried out.
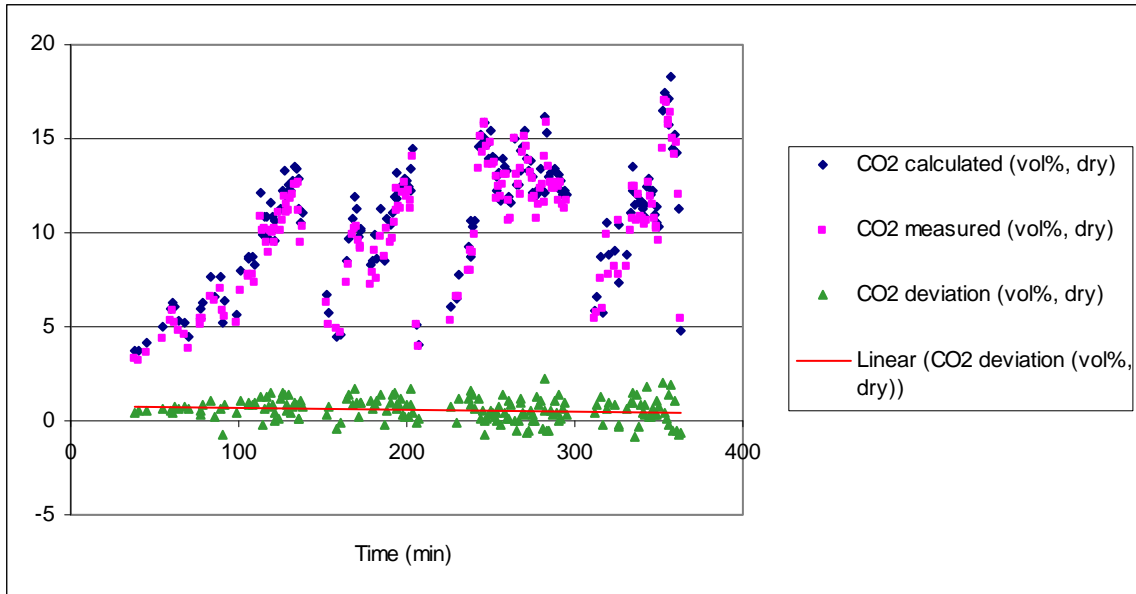
Figure 7 CO_2 and calculated CO_2 as a function of time (FTIR)
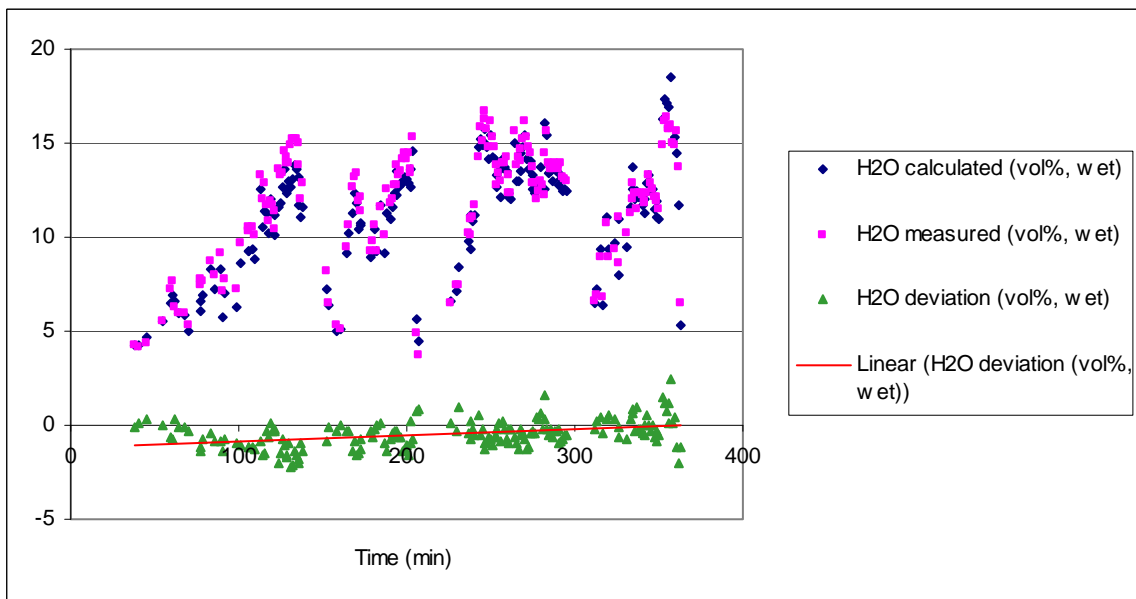

Figure 8 H_2O and calculated H_2O as a function of time (FTIR)

Emissions are presented as a function of excess air ratio and temperature. Emissions of NH_3, HCN, and HF are not reported due to the very low levels measured compared to the measurement uncertainty.

NOx emissions ($NO+NO_2$) at 11% O_2 in dry flue gas are shown as a function of excess air ratio in Figure 9 and as a function of temperature in Figure 10 for NOx measured by the Horiba analyzer. The conversion factor for fuel-N to NOx is shown in Figure 11. Clear excess air ratio dependence can be seen, while no significant temperature dependence can be seen. The large variation in the NOx emission level at each temperature level is due to the large excess air ratio variation introduced at each temperature level. The conversion factor for fuel-N to NOx lies between 0.08 (8%) and close to zero.
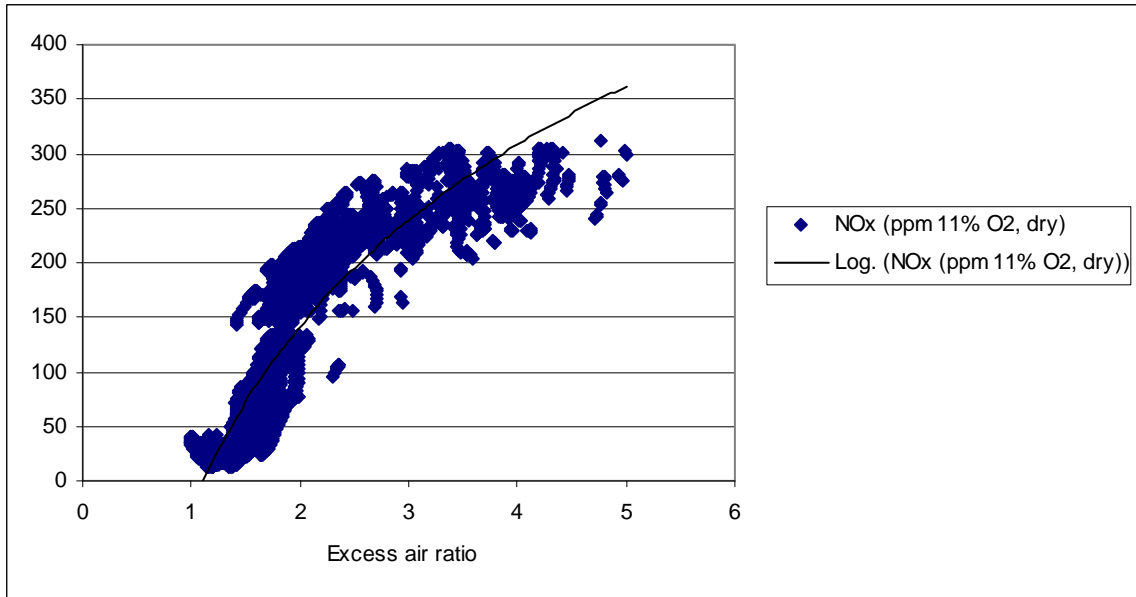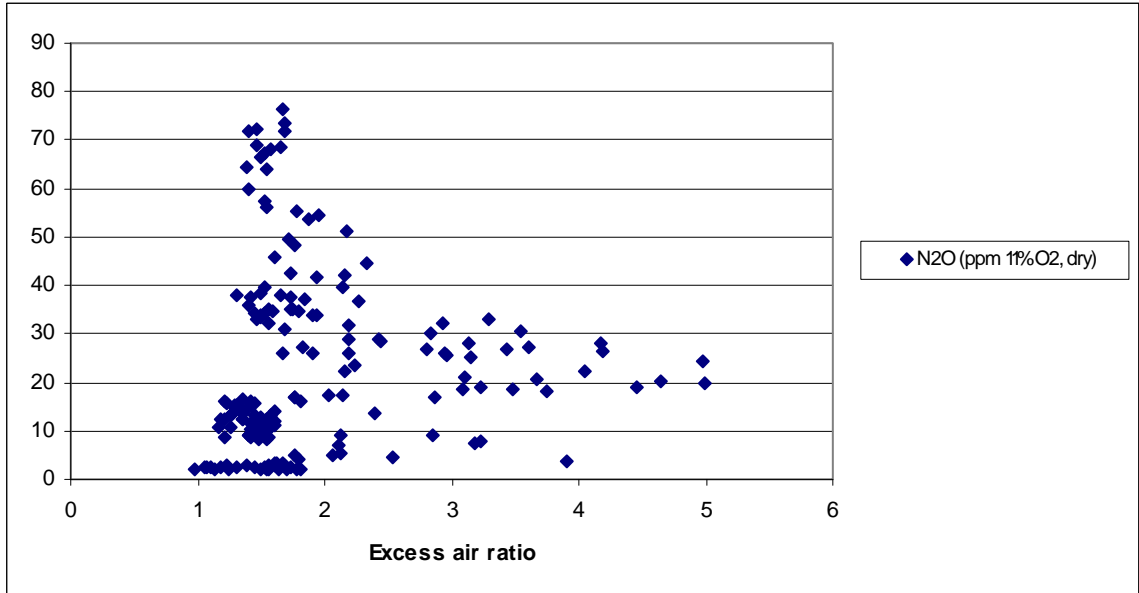
Figure 9 NOx emission level as a function of excess air ratio (Horiba)
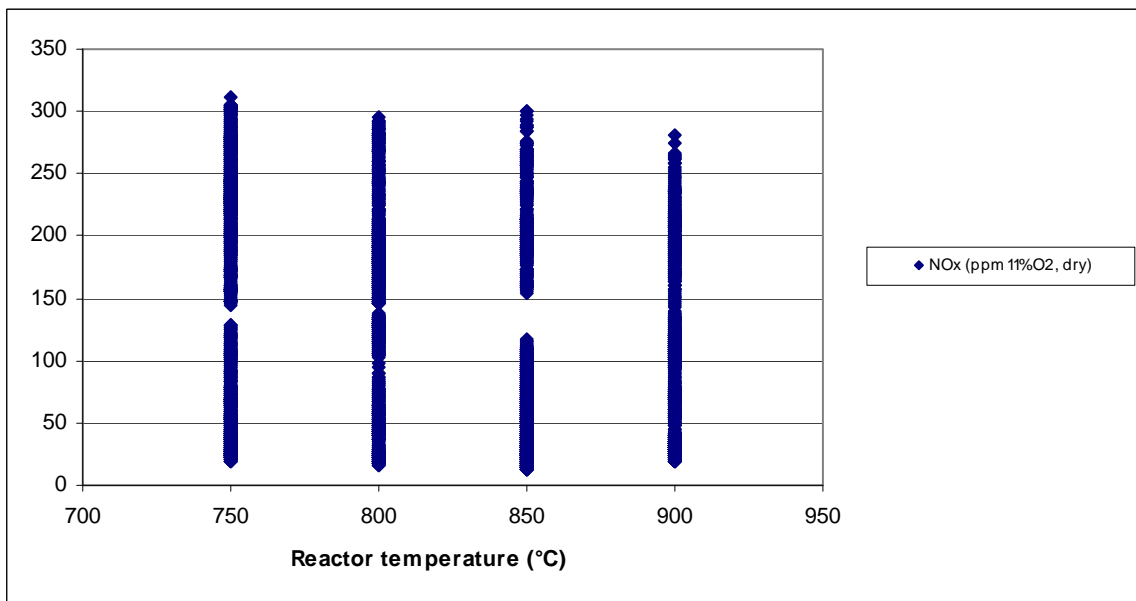
Figure 10 NOx emission level as a function of temperature (Horiba)
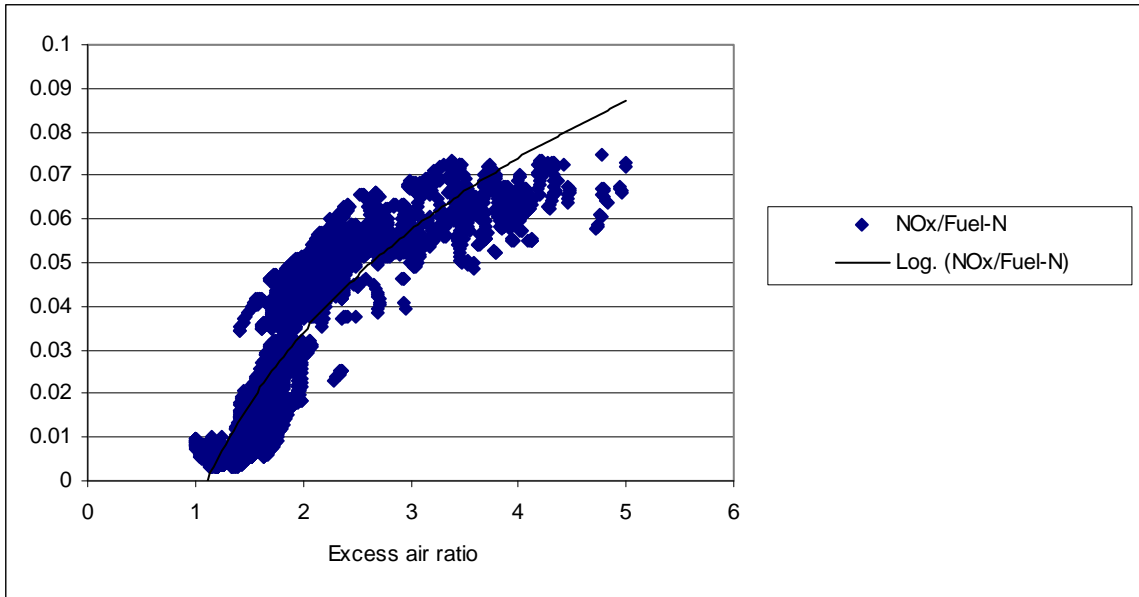
Figure 11 Conversion of fuel-N to NOx as a function of excess air ratio (Horiba)

N_2O emissions at 11% O_2 in dry flue gas are shown as a function of excess air ratio in Figure 12 and as a function of temperature in Figure 13 for N_2O measured by the FTIR analyzer. The N_2O emission level is relatively high at low excess air ratios and a clear temperature dependence of the N_2O emission level can as expected be seen.

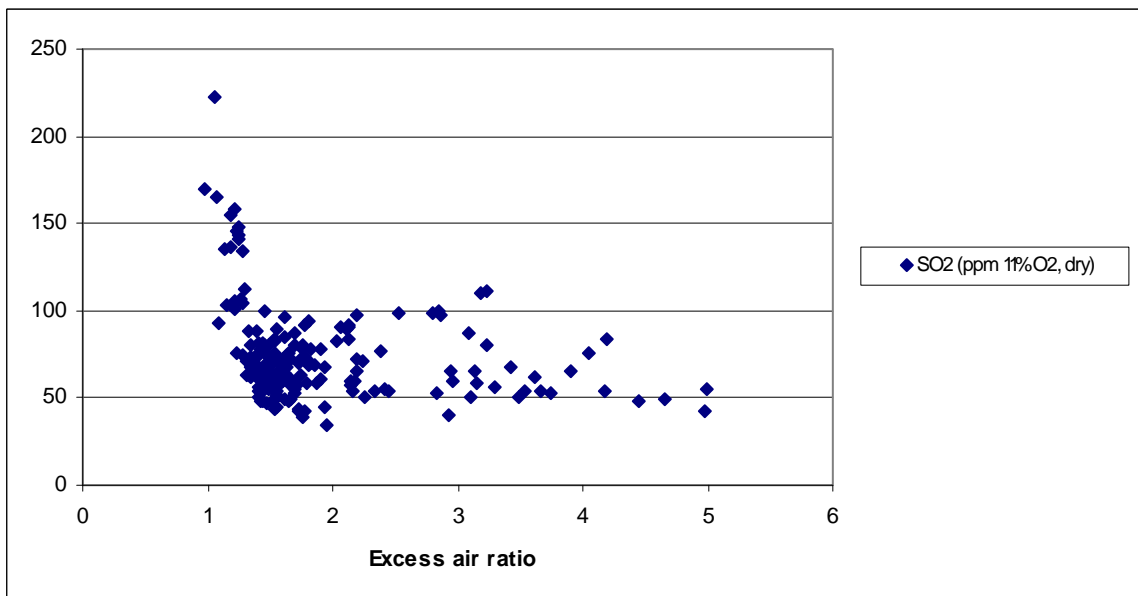**Figure 12 N_2O emission level as a function of excess air ratio (FTIR)**
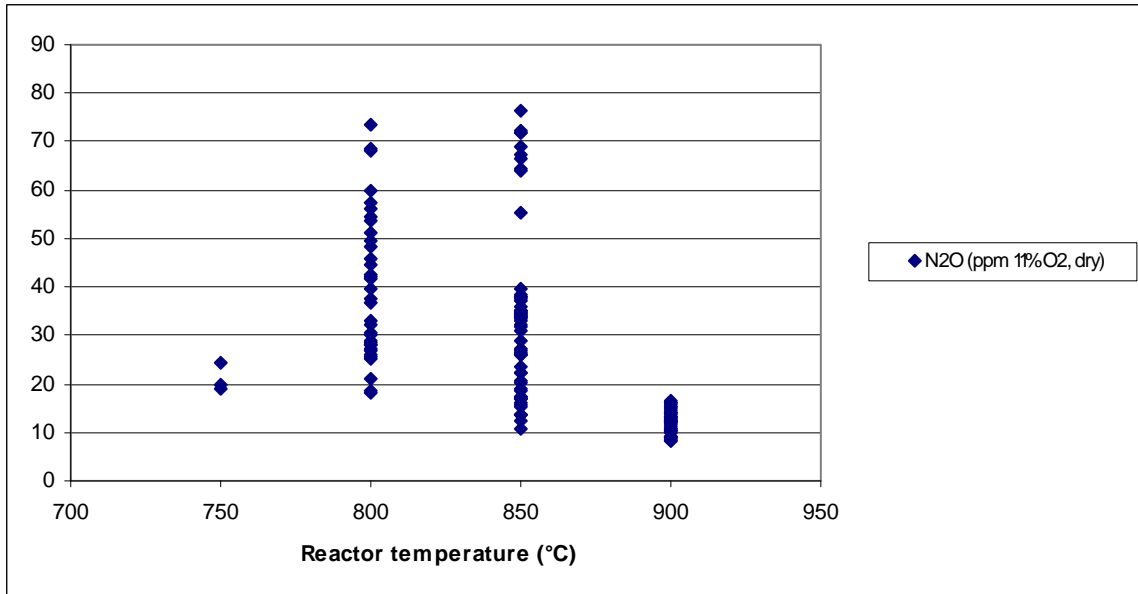
Figure 13 N$_2$O emission level as a function of temperature (FTIR)

SO$_2$ emissions at 11% O$_2$ in dry flue gas are shown as a function of excess air ratio in Figure 14 and as a function of temperature in Figure 15 for SO$_2$ measured by the FTIR analyzer. The conversion factor for fuel-S to SO$_2$ is shown in Figure 16. The SO$_2$ emission level is quite high, especially at very low excess air ratios. The conversion factor for fuel-S to SO$_2$ is too high, indicating that the fuel-S content in the peat is higher than given in the ultimate analysis, alternatively that the SO$_2$ measurements are too high. However, parallel SO$_2$ measurements in other similar multi-fuel reactor experiments shows good agreement with respect to the measured SO$_2$ emission level. Anyway, the influence of excess air ratio and temperature are not influence by the uncertainty in the fuel-S analysis. The SO$_2$ emission level decreases somewhat with increasing excess air ratio and increases with increasing temperature.

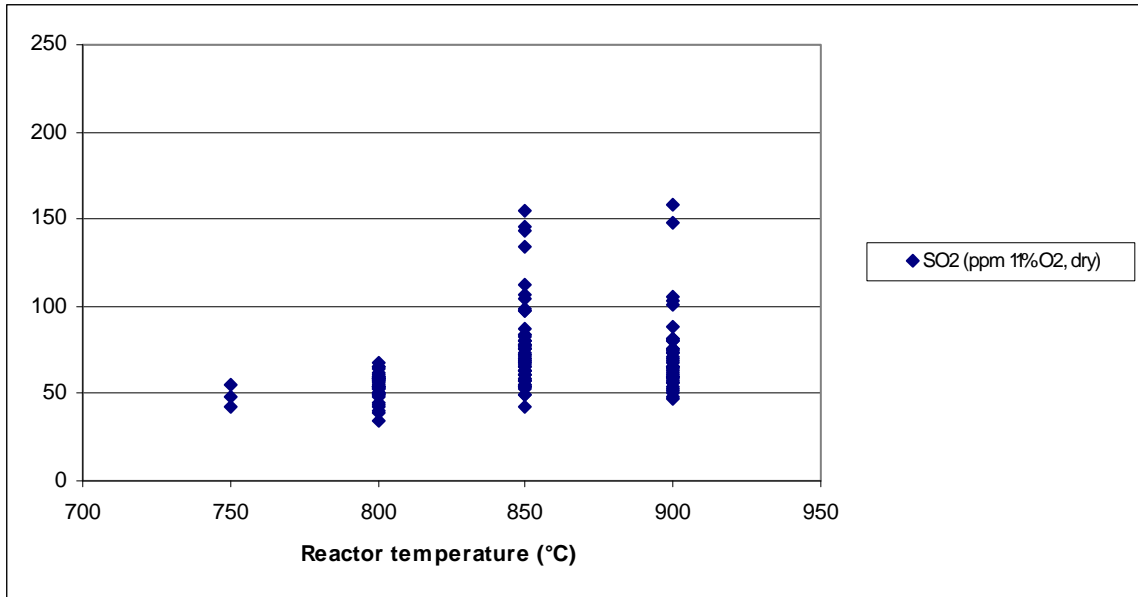**Figure 14 SO$_2$ emission level as a function of excess air ratio (FTIR)**

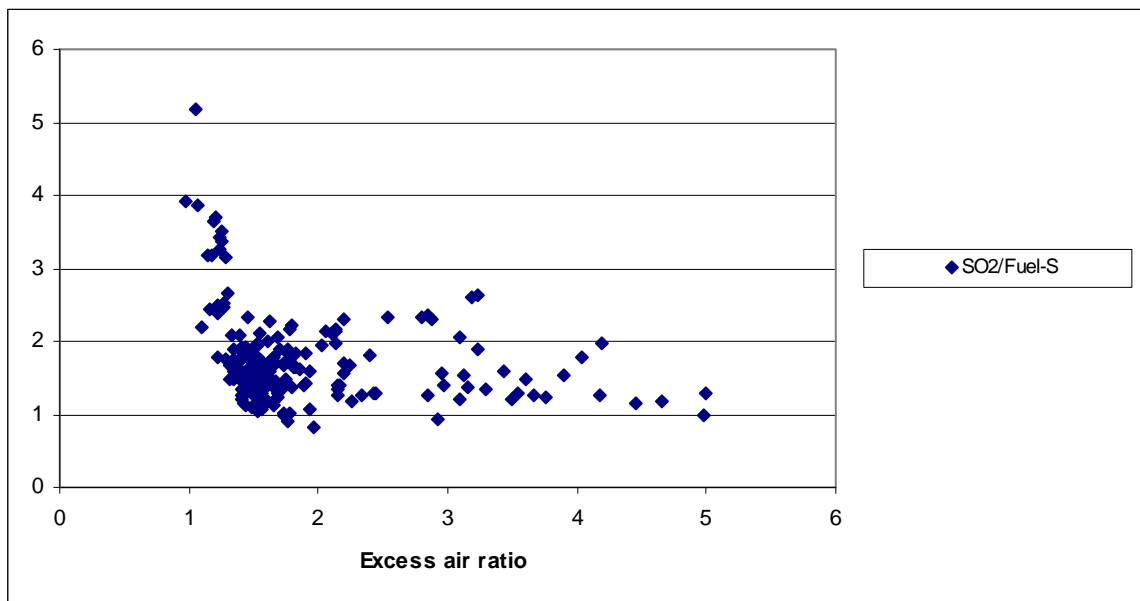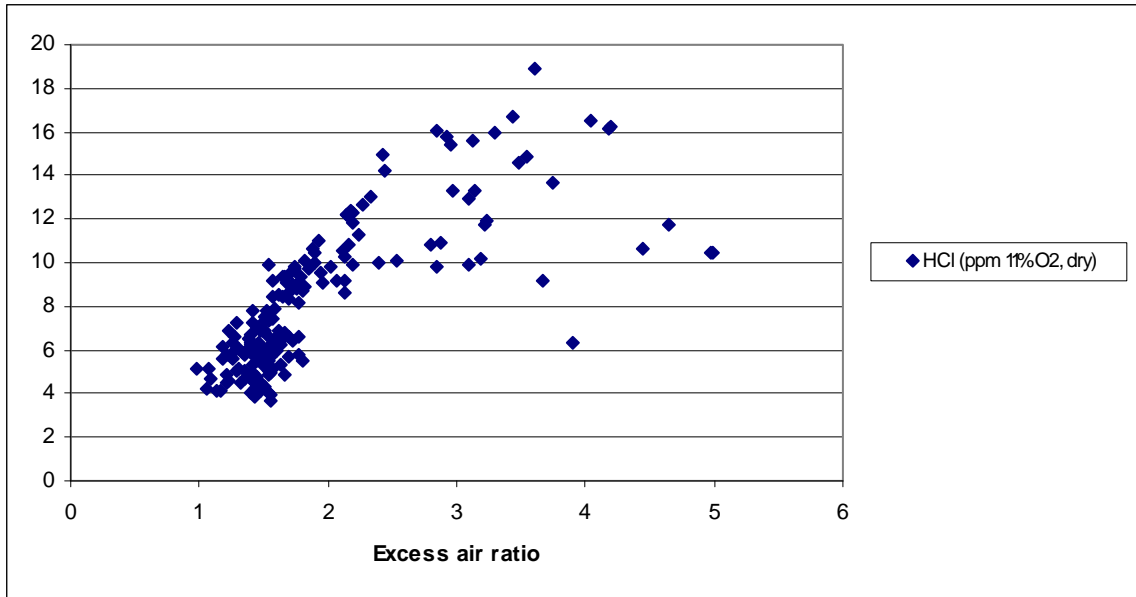**Figure 15 SO₂ emission level as a function of temperature (FTIR)**

Figure 16 Conversion of fuel-S to SO₂ as a function of excess air ratio (FTIR)

HCl emissions at 11% O₂ in dry flue gas are shown as a function of excess air ratio in Figure 17 and as a function of temperature in Figure 18 for HCl measured by the FTIR analyzer. The conversion factor for fuel-Cl to HCl is shown in Figure 19. The HCl emission level is increasing with increasing excess air ratio and shows a peak value as a function of temperature. The conversion factor for fuel-Cl to HCl lies between 0.35 (35%) and 0.05 (5%).

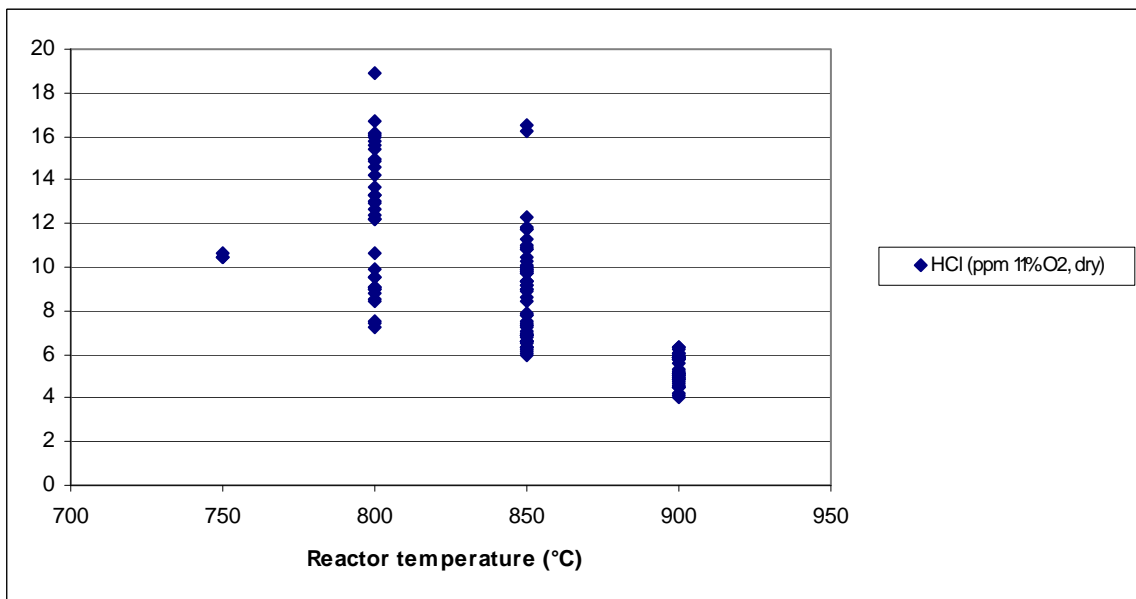**Figure 17 HCl emission level as a function of excess air ratio (FTIR)**

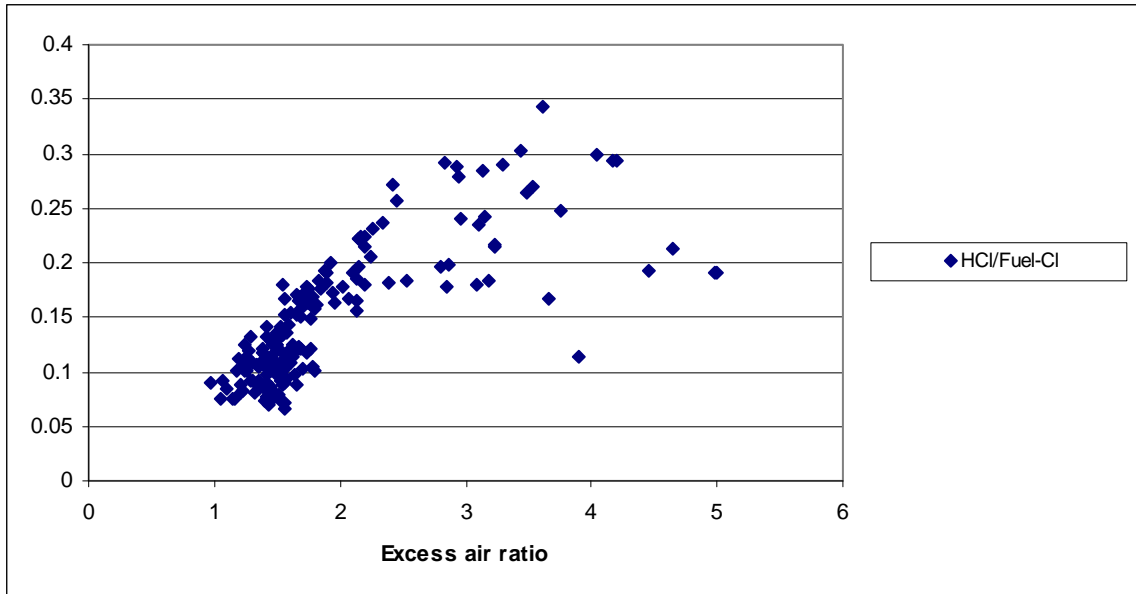**Figure 18 HCl emission level as a function of temperature (FTIR)**

Figure 19 Conversion of fuel-Cl to HCl as a function of excess air ratio (FTIR)

CO emissions at 11% O_2 in dry flue gas are shown as a function of excess air ratio in Figure 20 and as a function of temperature in Figure 21 for CO measured by the FTIR analyzer. A very low CO emission level can be seen except at very low excess air ratios, where limitations in local O_2 availability will limit the CO burnout, i.e. the CO emission level is a result of imperfect mixing conditions. The very low excess air ratios are typically seen at the highest temperature level where the fuel conversion rate and the O_2 consumption are at their highest values.
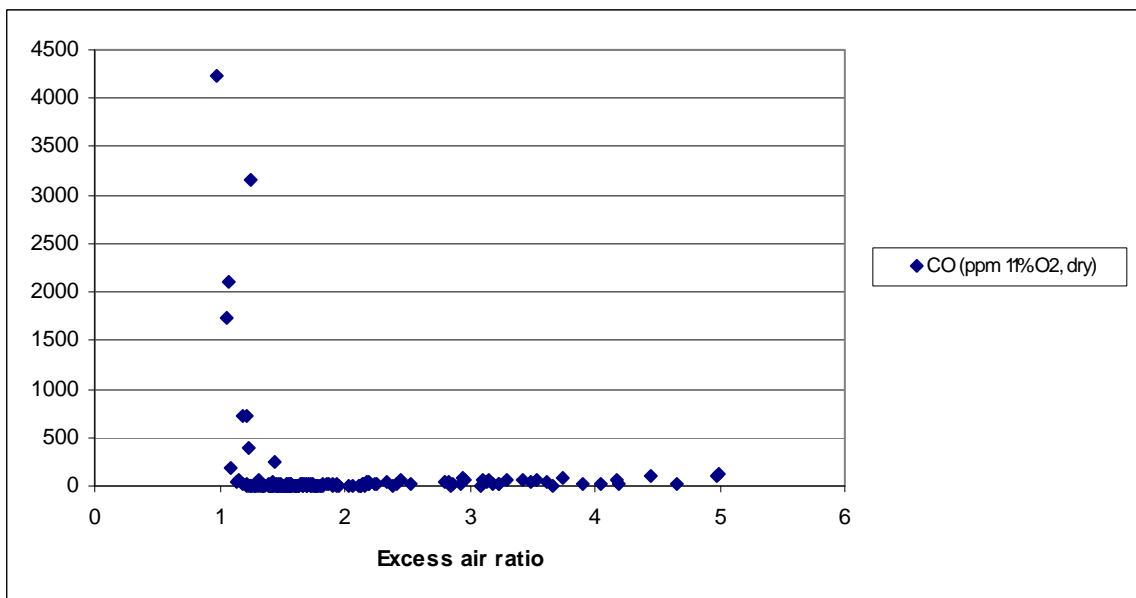

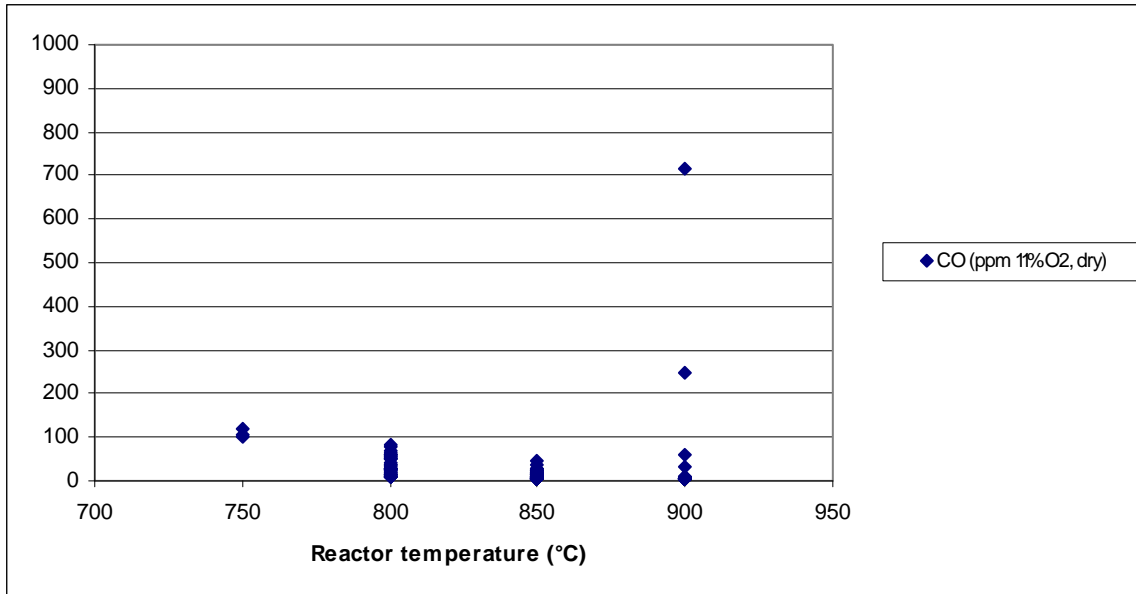**Figure 20 CO emission level as a function of excess air ratio (FTIR)**

Figure 21 CO emission level as a function of temperature (FTIR)

Hydrocarbons (CxHy) emissions at 11% O_2 in dry flue gas are shown as a function of excess air ratio in Figure 22 and as a function of temperature in Figure 23 for CxHy measured by the FTIR analyzer. As for CO, a very low CxHy emission level can be seen except at very low excess air ratios, where limitations in local O_2 availability will limit also the CxHy burnout, i.e. the CxHy emission level is a result of imperfect mixing conditions. The very low excess air ratios are typically seen at the highest temperature level where the fuel conversion rate and the O_2 consumption are at their highest values.
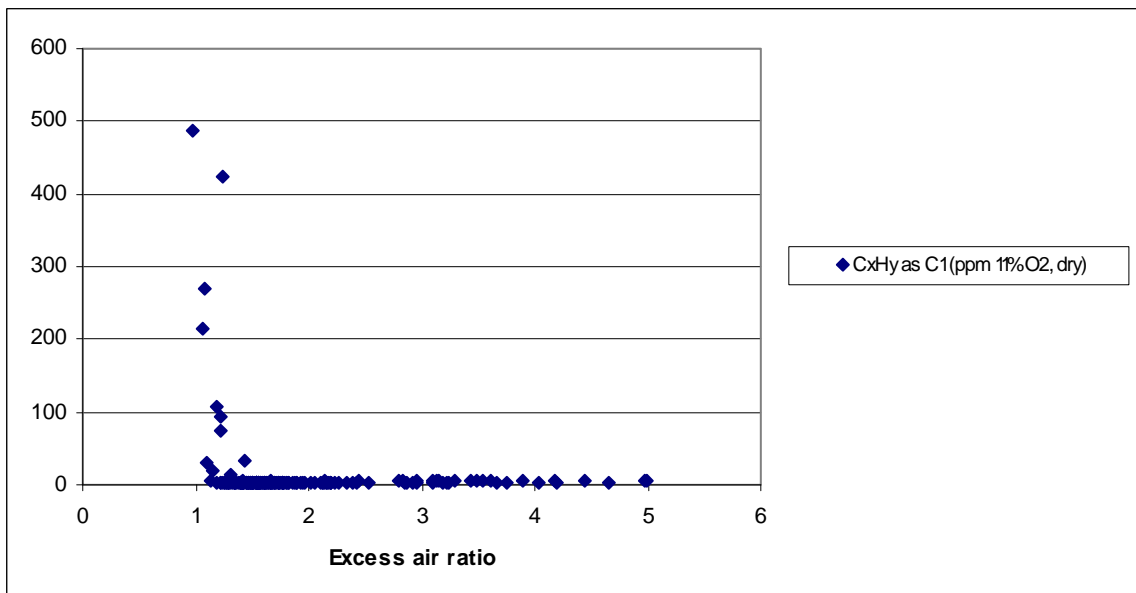

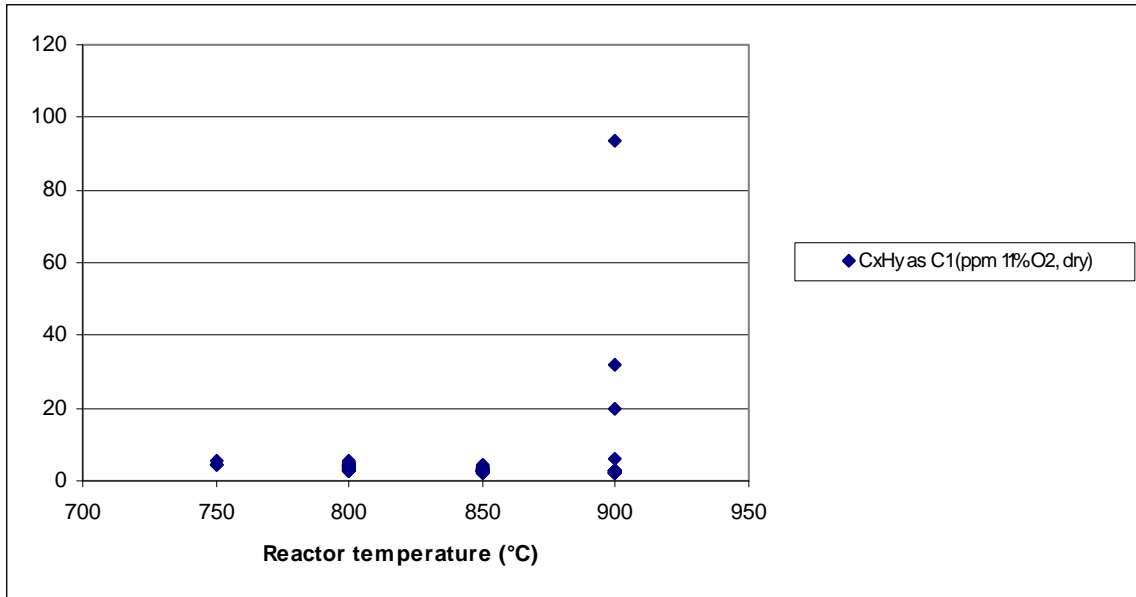**Figure 22 CxHy emission level as a function of excess air ratio (FTIR)**

Figure 23 CxHy emission level as a function of temperature (FTIR)

4 DISCUSSIONS

Comparing with similar experiments with wood and demolition wood [7], the thermal decomposition behaviour of peat is different as shown in Figure 24. Devolatilisation starts at a lower temperature for peat at both pyrolysis and combustion conditions and the amount of fixed carbon in the peat is higher. The chemical composition of peat is different from wood, giving a weight change curve as a function of temperature that differs from wood.
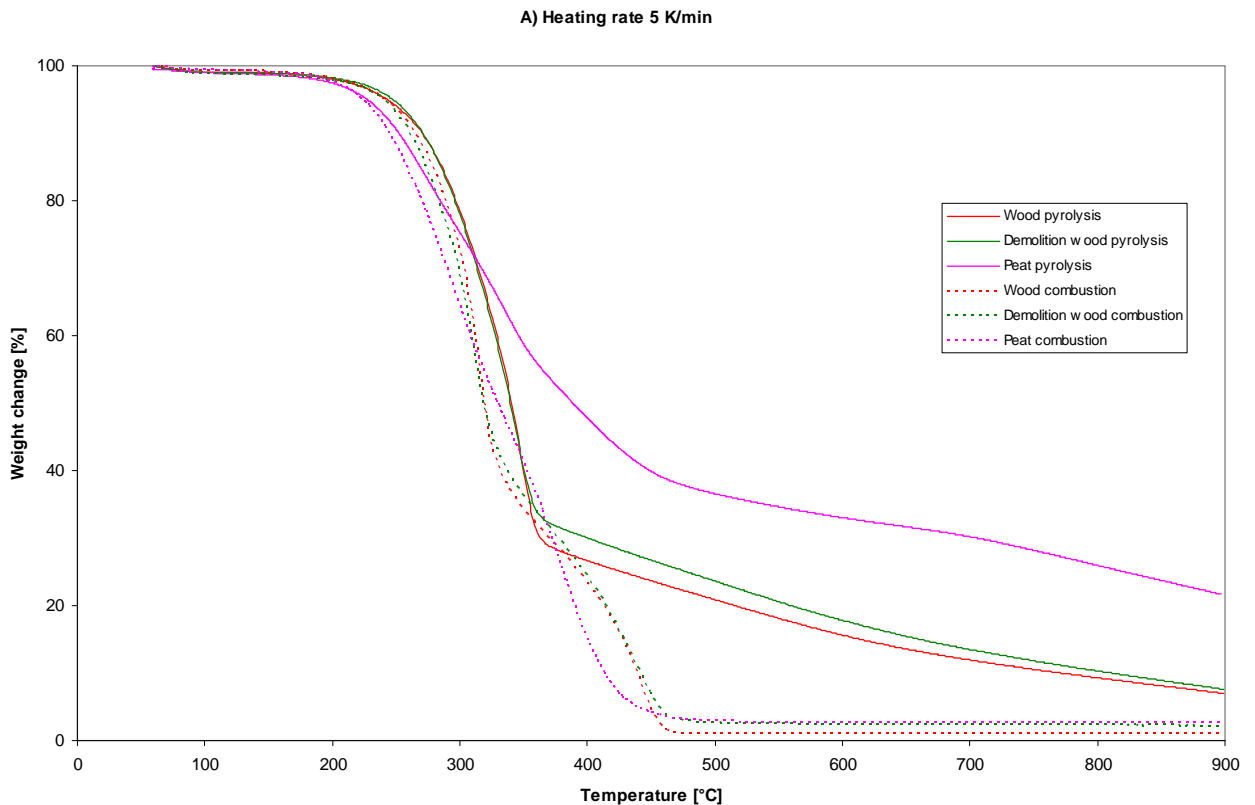
A) Heating rate 5 K/min

Figure 24 Peat TGA results compared to wood and demolition wood

Comparing with similar experiments with other fuels, the emission behaviour of peat is similar, but the high nitrogen content of the peat gives higher NOx and N_2O emissions compared to woody biomass. The SO_2 emission level from the peat is relatively high, while the HCl emission level is relatively low. As such peat has the potential to decrease corrosion and fouling in co-firing applications utilising poor quality biomass fuels containing high levels of chlorine in combinations with high levels of alkali metals.

5 REFERENCES

[1] Bergner K., Albano Ch.: Thermal analysis of peat, Anal. Chem., 1993, 65, 204-208

[2] Orru H., Kaasik M., Merisalu E., Forsberg B.: Health impact assessment in case of biofuels peat-Co-use of environmental scenarios and exposure-response functions, Biomass and bioenergy 33 (2009), 1080-1086

[3] Persson J-A., Johansson E., Albano Ch.: Quantitative Thermogravimetry on peat. A Multivariate Approach. Anal.Chem., 1986, 58, 1173-1178

[4] Prins J.M., Ptasinski K.J., Janssen J.J.G.: More efficient biomass gasification via torrefaction, Energy 31 (2006) 3458-3470

[5] Senneca O.: Kinetics of pyrolysis, combustion and gasification of three biomass fuels, Fuel Processing Technology 88 (2007) 87-97

[6] Sandquist J., Horrigmo W., Ortega M., Skreiberg Ø. (2009). The multi-fuel reactors setup at SINTEF Energy Research, TR A6824

[7] Sandquist J., Ortega M., Skreiberg Ø. (2008). Thermogravimetric investigation of four fuels, TR A6769